SYNTHESIS AND STUDY OF $CS_5H_3(SO_4)_4$ AND $(CS_{1-X}RB_X)_5H_3(SO_4)_4$ FOR INTEGRATION AS ELECTROLYTES IN SOLID ACID FUEL CELLS

[1]Jay Shah, [2]Chatr Panithipongwut, [2]Nicholas Scianmarello

AUGUST 29, 2009

[1]Texas Academy of Mathematics and Science
[2]California Institute of Technology

MENTOR: Dr. Sossina M. Haile
Professor of Materials Science and Chemical Engineering
California Institute of Technology
Pasadena, CA

Abstract: The most common type of fuel cell in today's industries is the Phosphoric Acid Fuel Cell (PAFC). While these fuel cells show potential, new research shows that Solid Acid Fuel Cells (SAFCs) offer several benefits over the more conventional PAFCs such as operation in an anhydrous environment and relatively low operating temperatures. $Cs_5H_3(SO_4)_4$ is a possible candidate for electrolytes in SAFCs because of its superprotonic conductivity and its functional temperature range. Previous research on $Cs_5H_3(SO_4)_4$ suggests the presence of a superprotonic phase at approximately 140 °C. We explored different synthesis methods of $Cs_5H_3(SO_4)_4$ and, based on our results, attempted to synthesize pure samples of $Cs_5H_3(SO_4)_4$ by small drop injection. For the first time, rubidium was integrated into the crystal lattice structure of $Cs_5H_3(SO_4)_4$ to observe changes in physical properties. Our results confirm the superprotonic phase suggested in previous research of $Cs_5H_3(SO_4)_4$ at 143 °C and shows similar superprotonic behavior in $Cs_{0.95}Rb_{0.05}H_3(SO_4)_4$ at 130 °C. We analyze our samples via methods of x-ray diffraction, thermogravitmetic analysis, differential scanning calorimetry, and AC impedance spectroscopy. Our results justify further exploration of $Cs_5H_3(SO_4)_4$ and $(Cs_{1-x}Rb_x)_5H_3(SO_4)_4$ as electrolytes in solid acid fuel cells due to their preferable operating temperature and high proton conductive nature.

Introduction

The desire to seek new methods to obtain energy has stimulated great interest in all fields of science, especially in fuel cells. Conventional fuel cells operate by diving H_2 atoms into their positive and negative components ($2H^+$ and $2e^-$) and exploiting their affinity. Fuel cells consist of an anode, cathode, and an electrolyte in which the anode separates the proton from the electron and the cathode reunites the two. The electrolyte functions to only permit protons through its membrane, forcing electrons to take an external path to the cathode, generating electricity in this process. Reunification of the hydrogen protons and electrons in the cathode occurs in the presence of oxygen in the air, which results in H_2 and O_2 atoms combining to make water. Electricity is harnessed from the work the electrons do by traveling through an external circuit before combining again with H^+ atoms at the cathode. This process, though conceptually rudimentary, is complicated by several prerequisites. High operating temperatures for certain fuel cells endanger long term reliability and require expensive high-temperature graded components in its architecture [1,6]. Furthermore, fuel cells such as phosphoric acid fuel cells (PAFCs) require a hydrated environment in order for successful proton conductivity, further increasing construction and operating costs.

As a result of these shortcomings in conventional PAFCs, Solid acid fuel cells (SAFCs) have recently been receiving great interest in the renewable energy field because of the several advantages they offer over conventional fuel cells. More specifically, solid acid fuel cells function in anhydrous environments and under low operating temperatures (100 °C to 250 °C) [2]. The liberation from a hydration maintenance mechanism is of significant importance and discontinues the need for complicated water management systems within the cell. The class of salts with the formula $M_5H_3(XO_4)_4$ (M = K, Rb, NH4, Cs; X = S, Se) are of great interest due to

their superprotonic conductivity and their potential as electrolytes in SAFCs [3]. Superprotonic conductivity is the increase in ionic conductivity by several magnitudes over a small temperature range. This conductivity is of critical significance because the unusually high proton affinity is a very desirable characteristic for electrolytes in fuel cells. Without this high conductivity, fuel cell efficiency would be significantly reduced. Previous research has defined high proton conductivity in $Cs_5H_3(SO_4)_4$ to the reorientation of SO_4 groups, creating vacancies in the hydrogen bond network and thus promoting proton transport [4]. This superconductivity is not present at room temperature, but occurs with slight heating. Conductivity was measured from 140 °C to 220 °C in which these crystals underwent phase transitions as well as dehydration. The yielded conductivity is consistent with previous literature and is as high as $\sigma \sim 10^{-2.5}$ $S \cdot cm^{-1}$.

X-ray diffraction played a key role in this study to analyze sample purity. X-ray diffractometers function by exposing test samples with x-ray beams and observing diffraction of these beams. Diffraction varies based on the crystal structure, or lattice, of a sample. Diffraction behavior can be explained by Bragg's law:

$$n\lambda = 2d(\sin\theta)$$

In this equation, n is an integer representing the order given, λ is the wavelength of the beam applied, d is the distance between layers in the lattice, and θ is the angle of incidence between the beam and the sample. Because the samples analyzed are crystals, they are composed of a repeating pattern and maintain the same distance, or d, between layers. The crystal structure varies from compound to compound, giving each compound's crystal structure its own unique "fingerprint". Because diffraction patterns are unique to each chemical compound, x-ray diffraction is an efficient method for crystal compound identification and purity analysis.

- Compound Synthesis

$$5\ Cs_2SO_4 \quad + \quad 3\ H_2SO_4 \quad \rightarrow \quad 2\ Cs_5H_3(SO_4)_4$$

In order to produce $Cs_5H_3(SO_4)_4$, henceforth referred to as Cs_5-, cesium sulfate and sulfuric acid were utilized in their stoichiometric amounts. All calculations were done to yield 5 grams of Cs_5-. The initial obstacle presented was determining which method of compound synthesis yielded the purest samples. Purity in this study is defined by the similarity to reference x-ray diffraction patterns, and therefore, similarity in crystal structure between reference and synthesized compounds. Previous literature in the subject prefers the synthesis method of crystallization [3,4], however other methods show potential of greater practicality. Four methods of compound synthesis were analyzed: thermal bomb, crystallization, precipitation, and small drop injection. Samples of Cs_5- from identical reactant amounts were synthesized using each of the methods above and analyzed for purity by means of X-ray diffraction. A Philips X-ray diffractometer (X'pert Pro) with Cu Kα radiation was used to analyze compounds for purity. All samples were analyzed at room temperature at an angular range of 10° to 80° (2θ) with a step size of 0.017° at 50.15 seconds per step. Purity was analyzed qualitatively by comparing the yielded patterns against a reference pattern attained from the Inorganic Crystal Structure Database [3] using *Philips X'pert Highscore* analysis software.

1.2 **- Procedure**

The thermal bomb procedure entailed mixing the reactants into an enclosed, high temperature suited container and then placing it in a furnace at 230 °C for 24 hours. Cs_2SO_4 (Alfa Aesar, 99.99%) was weighed into a plastic boat and then poured into the thermal bomb container. The weighing boat was lightly rinsed with water which was then also poured into the thermal bomb container in an effort to transfer all the Cs_2SO_4 into the reactant solution. H_2SO_4 (95%) was

weighed in a separate beaker and then transferred into the thermal bomb container by pipette. The contents of the thermal bomb container were stirred with a glass rod before being placed into the furnace. Special care was taken to use as minimal water as possible because excess water could not be removed once placed in the thermal container, resulting in a very thick and viscous solution. The container's lid was sealed tightly and placed in the furnace. After 24 hours, the container was removed carefully using heat resistant gloves and allowed to cool to room temperature before being opened. Thermal bomb samples tended to retain their moisture and were adhesive and gel-like. These conditions are not desirable for x-ray diffraction because samples need to be in a dry, powdered form. For this reason, samples were placed in an open container and kept in an oven at 100 °C for an additional 24 hours in an effort to dehydrate them.

The crystallization, precipitation, and small drop injection methods were all performed with a similar initial procedure. Cs_2SO_4 was carefully weighed in a plastic boat and then dissolved into small amount of distilled water ranging from 10-15 mL. H_2SO_4 was transferred into a beaker via pipette to weigh its appropriate amount. It was then poured into the Cs_2SO_4 + D.I. water solution. After transferring the H_2SO_4, its original beaker was rinsed with D.I. water and then poured into the Cs_2SO_4 + D.I solution as well. This ensured that there was not H_2SO_4 still remaining in the original beaker and all of the H_2SO_4 has been deposited in solution with Cs_2SO_4. Due to the difference in density, the water accumulated at the top of the solution. This (excess) water was evaporated by placing the beaker on a hot plate at medium heat (60-90 °C) for approximately 10 minutes, leaving the solution primarily consisting of the two original reactants; Cs_2SO_4 and H_2SO_4.

For crystallization, the beaker of reactant solution was kept on a hot plate until the sample started to crystallize. Crystallization was considered to have begun once small translucent rings

of 2-3 cm in diameter started to form at the surface of the solution. Once crystallization had begun, the beaker was removed from the hot plate and the crystal(s) were re-dissolved with the addition of 1-5 mL of water. They were then allowed to crystallize naturally by evaporation at room temperature. By first evaporating the water and then re-dissolving the crystal, excess water is removed from the solution, expediting the crystallization process and keeping only the minimal amount of water in the solution. A crystal required a range of 1-5 days to form depending on the amount of water removed from the system. Once the crystallization process was complete, the crystal was carefully removed with tweezers and rinsed off with distilled water to ensure that it did not have any impurities on its surface. Crystals were then placed in an oven for 24 hour at 100° C after which they were grinded to a powder in order to perform x-ray diffraction analysis.

In the precipitation method, the 10 – 15 mL solution (that remained after the excess water was evaporated) was exposed to a precipitating agent. A 200 mL solution of organic solvent (acetone 99%) was prepared in order to facilitate precipitation with the Cs_2SO_4 and H_2SO_4 (reactant) solution. An approximate ratio of 1:10 was maintained in the volume of the reactant solution and the volume of the precipitating solvent. The reactant solution was then slowly poured into the acetone, inducing precipitation. The solution was stirred for 15 minutes in order to allow the precipitate to collect at the bottom of the beaker. Precipitate was separated by means of filtration with a Buchner Funnel (150 Medium) and deposited into another flask. The flask was attached to a vacuum below the funnel to increase the rate at which the acetone and precipitate traveled through the filter. Precipitate was placed in an oven at 100° C for 24 hours to allow the sample to thoroughly dry. Following drying, the precipitate was grinded to a fine powder form in order to prepare for x-ray diffraction analysis.

In small drop precipitation, the reactant solution was also exposed to acetone. However, a micropipette was utilized to transfer the solution as opposed to depositing it all at once in acetone (as in the previous method of precipitation). The same ratio of 1:10 was maintained between the reactant solution and solvent. The solution was transferred to allow each droplet to make contact with the acetone individually, ensuring maximum surface area exposure to the precipitating solvent (acetone) and thus, yielding maximum precipitate. An identical procedure to that used in the precipitation method was used to extract the precipitate and prepare it for analysis via x-ray diffraction.

1.3 - **Overview of Synthesis Methods**

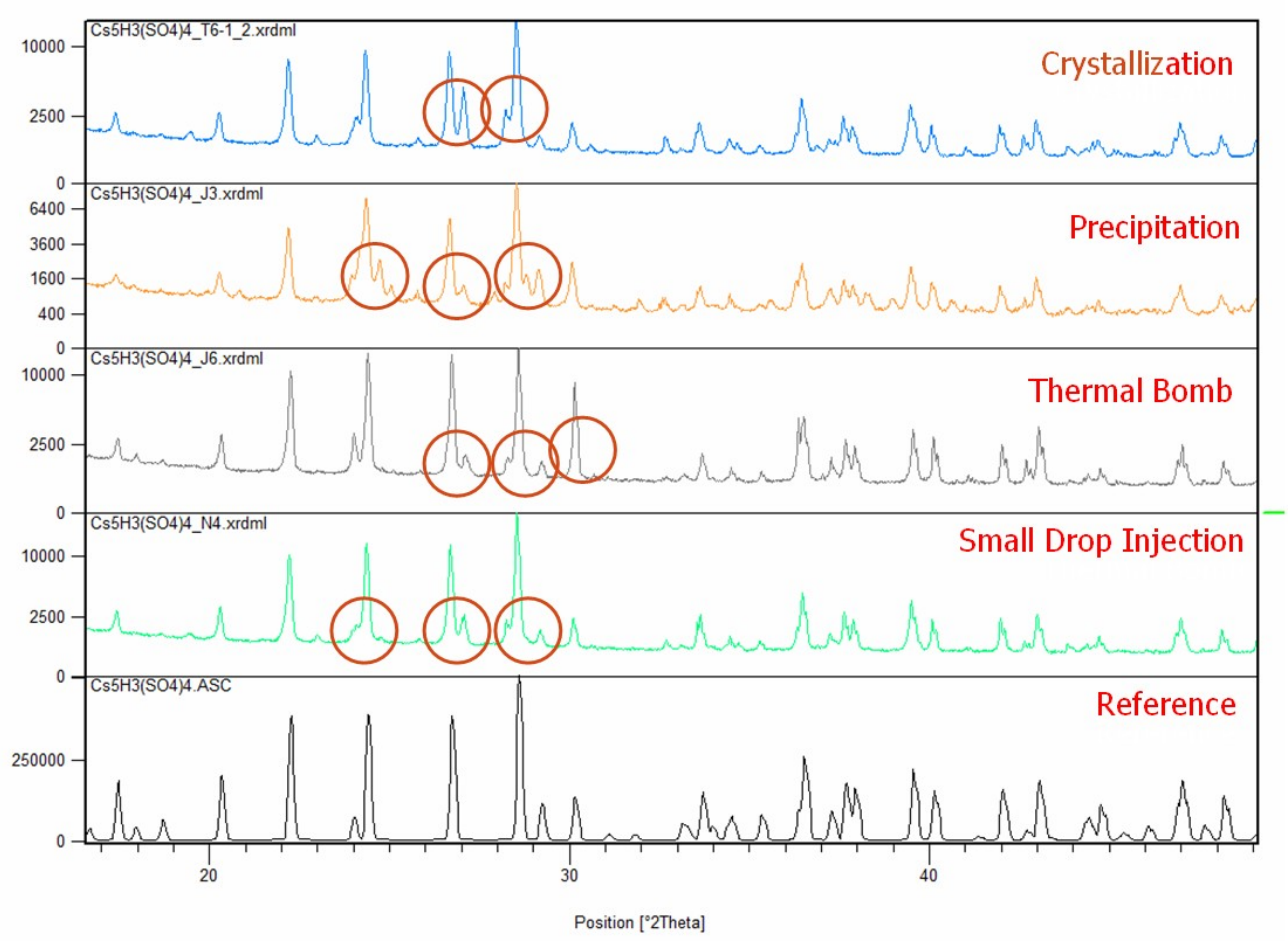

Figure 1: The results from x-ray diffraction are compared side by side against the reference pattern

Once synthesized and analyzed by x-ray diffraction, the yielded reference patterns were compared side by side against the reference pattern to determine similarity and degree of purity. Figure 1 shows peaks from 17 to 49 degrees, the range which contained the greatest variation in peak intensity and shape among the five patterns. Significant deviations from the reference pattern are highlighted. The results indicate that of the four synthesis methods, thermal bomb and small drop injection provide the greatest similarity between experimental and reference patterns. Crystallization and precipitation both show the presence of several extra minor peaks that are not

present in the reference pattern. The difference in purity between precipitation and small drop injection is substantial; the amount of surface area exposed to the precipitating solvent played a significant role in the sample purity. The thermal bomb pattern shows a significantly greater peak intensity at 30 degrees than that present in the reference sample. Furthermore, the thermal bomb procedure was significantly more difficult to reproduce in comparison to small drop injection. Specifically, the thermal bomb container was too heavy to be used on a balance and required all of the reactants to be measure in a separate container and then transferred into the thermal bomb. This is tedious because transferring a very specific amount of liquid via pipette is very difficult and has several sources of error. Additionally, thermal bomb sampled required a day longer in duration to be ready to analyze. Based on this reasoning, small drop injection was deemed as the most practical method and used as the sole synthesis method for the remainder of the study.

1.4 – **Enhancing Compound Purity**

Reactant amounts required calculation beyond stoichiometric ratios to account for sample impurity and proton retention. When stoichiometric amounts of reactants failed to provide pure samples, several variations in reactant amount were tested (up to ± 10% of the Cs_2SO_4 stoichiometric amount). After multiple tests, incremental deficiencies in the metal ion (Cs_2SO_4) presented increasingly pure samples of Cs_5-. We hypothesize that due to the high solubility of H^+ ions, slightly less amounts of Cs_2SO_4 were required to yield a sample in the Cs_5- phase (as opposed to $CsHSO_4$ or Cs_2SO_4) to compensate for small amounts of H^+ ions dissolving in the acetone instead of precipitating to form product. In other words, the dissolution of H^+ ions into acetone theoretically decreased the amount of H_2SO_4, which required a further reduction in the

amount of Cs_2SO_4. Within a set of samples synthesized with 1-3% deficiency of Cs_2SO_4, 2% Cs_2SO_4 deficiency showed the greatest resemblance to the reference pattern of Cs_5-.

1.5 – **Rubidium Integration**

The motivation behind rubidium incorporation is to observe changes in behavior and physical properties of the sample. Previously, rubidium compounds have been heavily researched for integration into fuel cells and such compounds belong to the same class of salts referenced to in the introduction of this paper; $M_5H_3(XO_4)_4$. Similar classes of compounds that have been researched with rubidium include RbH_2PO_4, $RbH_5(PO_4)_2$, and $Rb_3H(SO_4)_2$ [5][7]. These previous studies present superprotonic conductivity in rubidium compounds as well. Therefore, it was also postulated that integrating both cesium and rubidium into the lattice structure could yield a hybrid between Cs_5- and previously studied rubidium compounds. Thus, rubidium integration was attempted. Rubidium integration means that that the crystal structure of the $(Cs_{1-x}Rb_x)_5H_3(SO_4)_4$ sample is (theoretically) the same as $Cs_5H_3(SO_4)_4$, allowing the same parameters of x-ray diffraction to be used to analyze both Cs_5- and $(CsRb)_5$-. The purpose of maintaining the same lattice structure is due to the fact that the structure for Cs_5- is already efficient for proton transport; the reorientation of the sulfate groups (SO_4) attribute to this conductivity [4]. By maintaining the same crystal structure, we are not altering the vehicle the compound utilizes to generate proton transport.

$(Cs_{1-x}Rb_x)_5H_3(SO_4)_4$ was synthesized by beginning with the composition of the pure Cs_5- sample synthesized (2% metal deficiency) and substituting Cs with Rb in varying amounts. Of the various compounds tested, $(Cs_{0.95}Rb_{0.05})_5H_3(SO_4)_4$ resembled the reference pattern the greatest. This sample was synthesized with 6% metal ion deficiency, meaning there was 6% less of $(CsRb)_5$- than the stoichiometric amount. This deficiency was a result of a “trail and error”

process during the process of yielding a pure sample. Similarly to the process of synthesizing a pure Cs_5- sample, different amounts of reactant ratios were tested to see the result in overall sample purity. Published studies state the lattice parameters for the Cs_5- sample compound are a=b=6.237(1) Å, c=29.613(2) Å[3]. Computer analysis with *Philips X'pert Plus* showed that our purest sample of $(CsRb)_5$- has lattice parameters of a=b= 6.2261 Å and c = 29.546 Å. This strong similarity in lattice parameters validated further investigation of this compound's physical and electrical properties.

2.1 – **Sample Analysis**

In order to gain understanding of each sample's behavior, samples were analyzed by means of thermogravitmetic analysis, differential scanning calorimetry, and AC impedance spectroscopy in addition to x-ray diffraction. The combination of these tests allows structure and behavior to be observed as a function of temperature.

Thermogravitmetric analysis (TGA) measures the change in mass in relation to change in temperature. This method of study provides valuable insight in crystal organization in that structural changes often involve an increase or decrease in mass. For example, changes such as dehydration induce a reduction in mass due to moisture being removed from the compound. Differential scanning calorimetry (DSC) measures heat flow as a function of temperature. Specifically, it measures energy required to increase and decrease the temperature of a sample. This test is done simultaneously with TGA and is useful because phase transitions are noted in these tests by exothermic (melting) and endothermic (solidification) peaks. Structural changes in a compound will also be revealed in DSC as a compound's specific heat depends on its structure because a compound will absorb heat at a different rate after it undergoes a phase transition, regardless if it changed state of matter or not. 40 mg of Cs_5- and 80 mg of $(CsRb)_5$- were analyzed

using a Netzsch-Jupiter STA 449C furnace and Netzsch TASC 414/4 Controller. Samples were tested from room temperature to approximately 300 °C.

AC Impedance provides conductivity measurements at different frequencies and temperatures. Single frequency tests were performed under humidified nitrogen on samples at a range of temperatures in order to determine when the superprotonic activity occurs. Approximately 0.350 grams of sample was pressed into a pellet under 1.25 tons of force for 5 minutes. Pellets were then sanded on both sides to reduce the total thickness by 0.2 mm and then applied with Pelco silver colloidal paste (Product No: 16032) on both sides to fulfill the role of electrodes. Pellets were 10 mm in diameter and about 1.5 mm in thickness. An Agilent Precision LCP Meter (4284A), Barnstead Electrothermal boiler, and Carbolite furnace were employed to measure conductivity. Cs_5- and $(CsRb)_5$- samples were tested from 120 °C to 230 °C and 100 °C to 210 °C, respectively at 45 kHz and with a voltage of 50 mV.

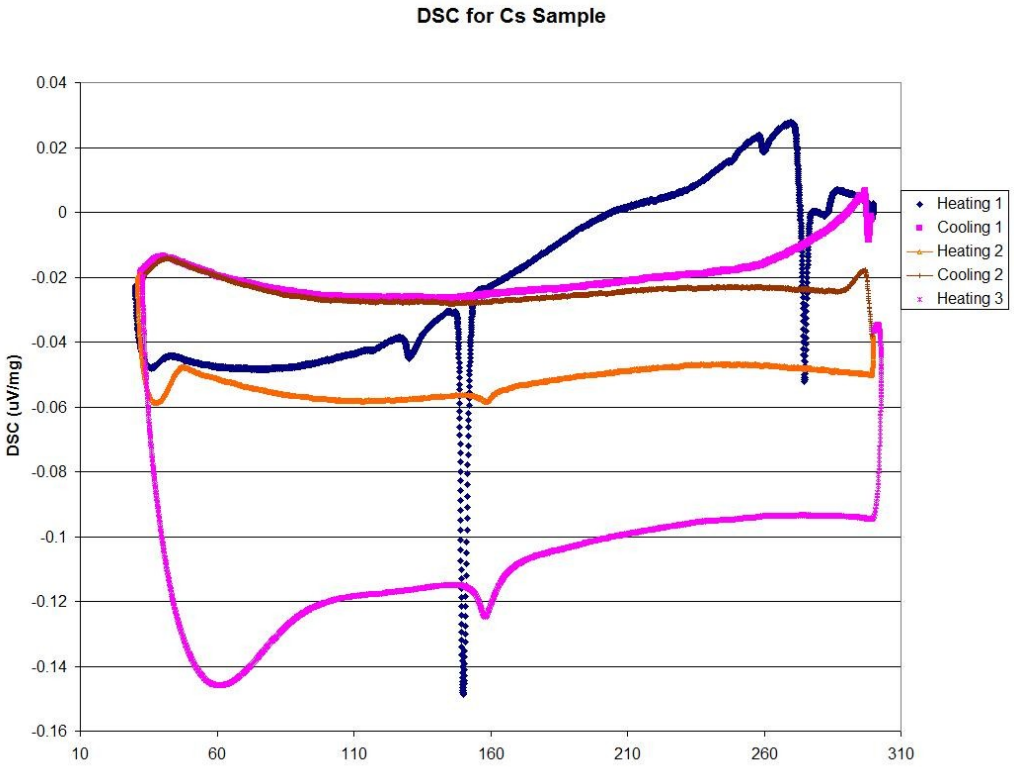

Figure 2: In each of the runs, an exothermic peak is observed at approximately 150 °C. On the first heating cycle, an exothermic peak is noted at 270 °C.

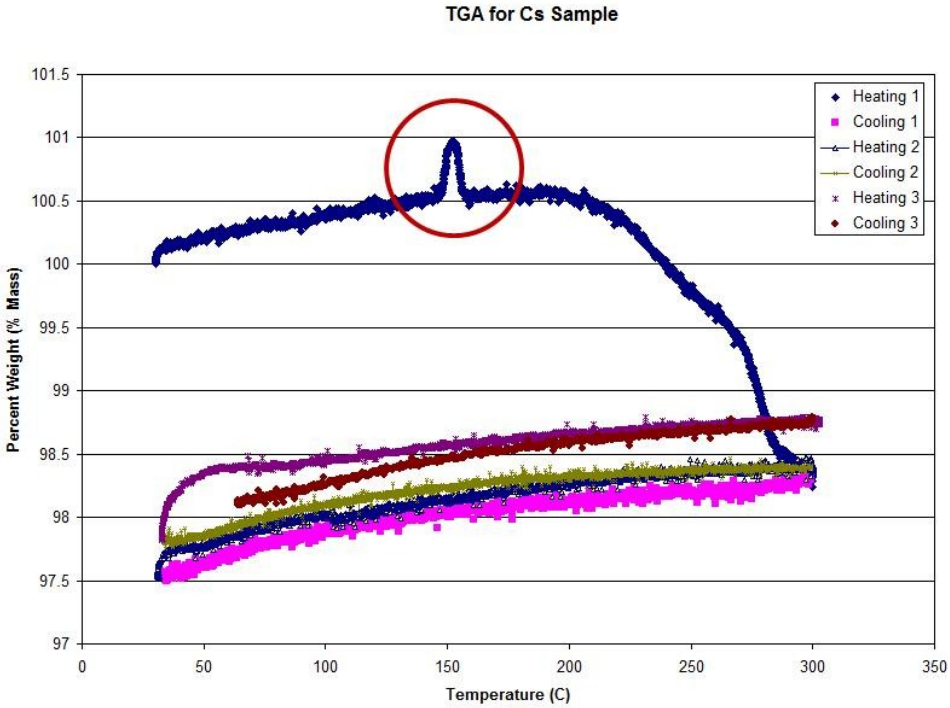

Figure 3: A unexpected peak at 150 °C is highlighted. This peak was concluded to be erroneous because it is inconsistent with the rest of the data; this peak only occurs in one heating cycle and there is no supporting data to correlate with an increase in mass. Furthermore, this increase in mass is not consistent and resumes to normal level very quickly.

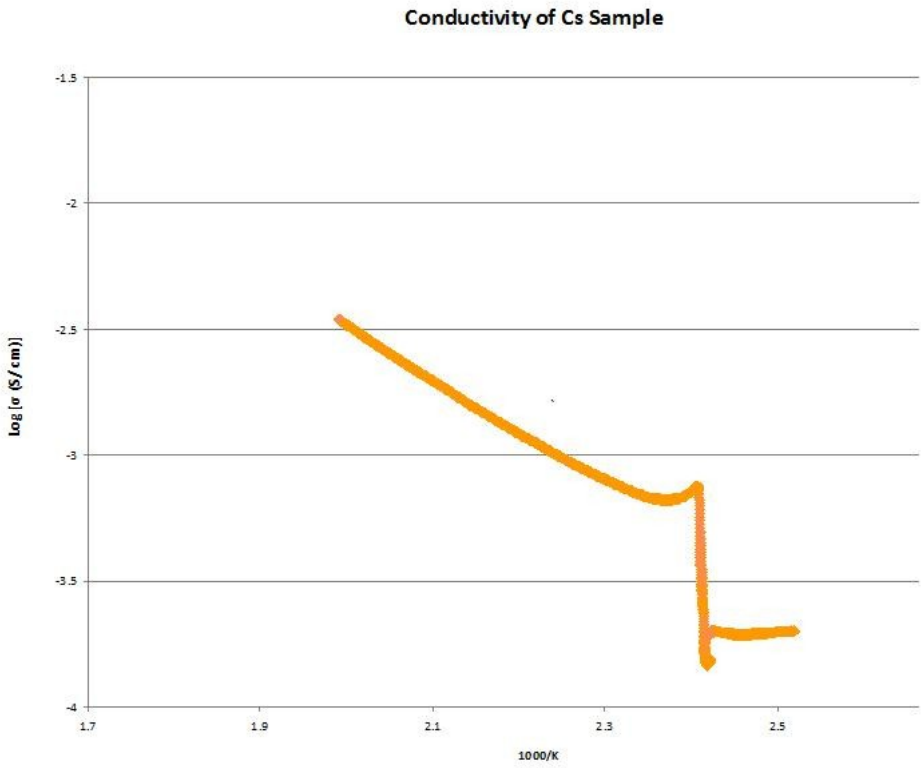

Figure 4: The superprotonic phase can be seen at 140 °C (X = 2.4).

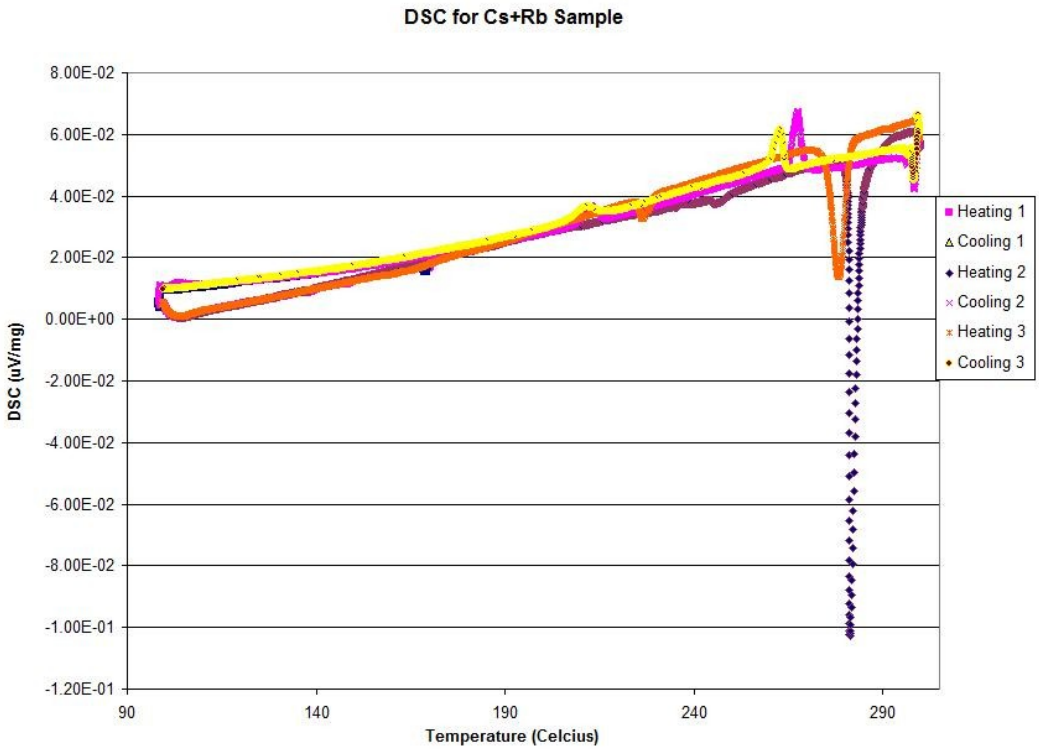

Figure 5: No significant peaks are experienced until 200 °C and 280 °C. Very minor peaks are observed at 170 °C.

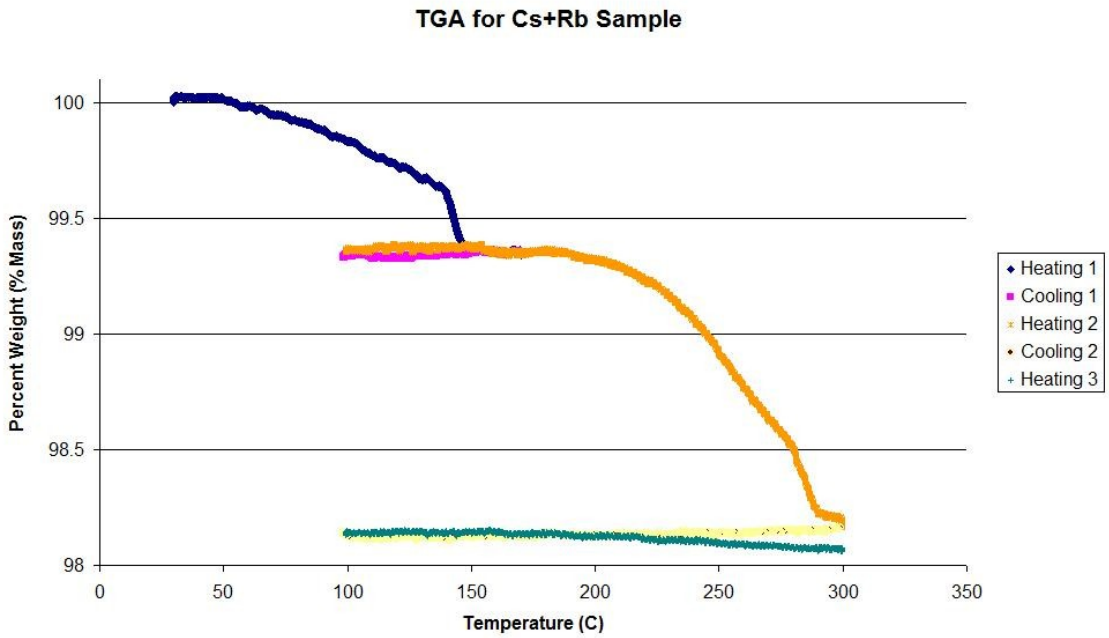

Figure 6: Large dehydration occurs in two separate steps from 100 °C to 280 °C, evidenced by the occurrence of two subset decreases in mass.

Figure 5: No significant peaks are experienced until 280 C. Very minor peaks are observed at 140 C.

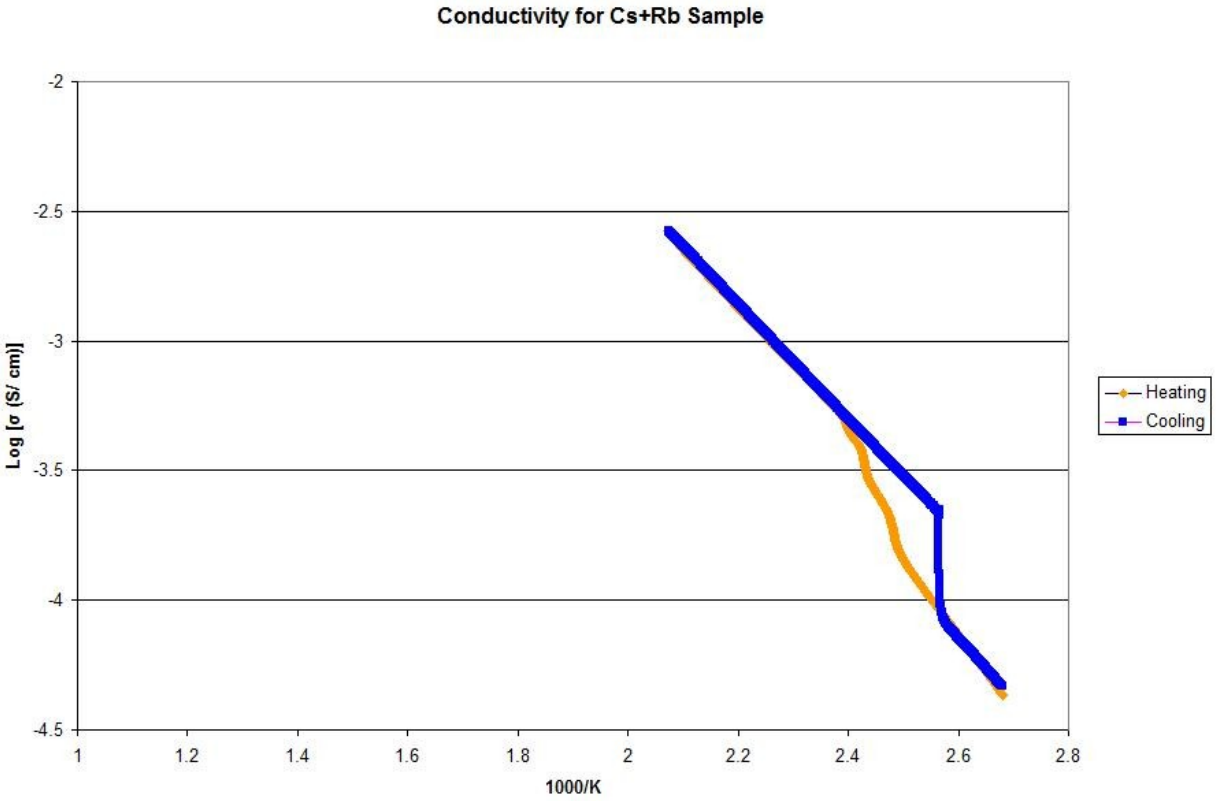

Figure 7: Superprotonic activity is suggested due to the sharp decline of conductivity in the cooling phase, however, the heating phase fails to reciprocate this evidence. While this chart fails to show a superprotonic phase, the existence of this phase is strongly suggested by the data presented in the cooling phase.

3.1 – **Results**

The DSC graphs of Cs_5- show a strong exothermic peak at 145 °C. This indicates a phase transition because this exothermic peak is consistently present in the multiple heating runs. The exothermic peak present at 270 °C only appears once. This peak can be attributed to dehydration since a sample can only dehydrate once; once moisture is lost in a sample, it will not be regained. The TGA analysis shows a steady loss in mass from 200 °C to 300 °C in the first run which it never recoups, supporting the dehydration hypothesis. The TGA graph also shows an error at 150 °C; an acute increase in mass. This peak is not to be confused with the phase transition present at 145 °C because this peak only occurs once and phase transitions do not necessarily induce changes in mass. Furthermore, TGA machines are extremely sensitive and subject to errors in their results if there is significant activity, such as movement, present in the machine's surroundings. Because these tests were not run in an isolated environment, errors such as this peak in the TGA results are not unexpected. To maintain integrity in the results, the graph was not corrected for this error.

Superprotonic conductivity occurs in the Cs_5- sample at the same approximate temperature at which it undergoes a phase transition; 145 °C. Previous literature attributes this phase transition/conductivity to a change from space group P63/mmc phase II to group P6/mmm, phase I [3]. Hence, this phase transition is the cause of the superprotonic conductivity.

The $(CsRb)_5$ graphs showed very interesting results. In the DSC graph, only one significant exothermic peak is shown at 280 °C and one very minor endothermic peak is present at 200 °C. The TGA graph for $(CsRb)_5$ shows a steady dehydration from 100 °C to 300 °C. Just as in the Cs_5- sample, this decrease in mass can be attributed to dehydration because sample weight does not increase back to the level in which the test started.

Superprotonic conductivity is suggested, but is not accurately portrayed in the $(CsRb)_5$ sample. On the heating portion of the conductivity test, the sample fails to exhibit superprotonic behavior. However, during the cooling cycle, the conductivity is reduced by several magnitudes as temperature decreases. This rapidly decreasing conductivity is a reciprocal indication of superprotonic activity; rapid decrease in conductivity during cooling should follow rapid increase in conductivity during heating. Even though conductivity results fail to show this, we still hypothesize that this sample has a superprotonic phase. Due to time constraints, further tests have not yet been run.

4.1 – **Conclusion**

Our initial study of synthesis methods provided an improved and more efficient way to synthesize crystals. Previous studies, regarding both Cs and Rb compounds as electrolytes, strongly prefer the crystallization method. Through several tests and comparisons in x-ray diffraction patterns, we show that small drop injection is the most effective method of compound synthesis. Not only does small drop injection yield a more pure sample, but it is also a quicker method of synthesis, especially in comparison to crystallization.

Our synthesis of $Cs_5H_3(SO_4)_4$ is consistent with previous studies[3] in that it exhibits superprotonic activity at 145 °C when it undergoes a transition from space group P63/mmc phase II to group P6/mmm, phase I[3]. Furthermore, we conclude that at 270 °C, it experiences a dehydration phase. With the confirmation of high proton conductive behavior, the next step of this study would be to more directly integrate $Cs_5H_3(SO_4)_4$ into a fuel cell environment.

Our study of $(Cs_{0.95}Rb_{0.05})_5H_3(SO_4)_4$ evidenced the presence of a superprotonic phase at approximately 130 °C. Furthermore, two dehydration phases are present in this compound from 100-150 °C and 200-280 °C as suggested by the two decreases in mass in the TGA results. DSC

results show a minor peak is present at 170 °C and a major peak at 280 °C. The peaks shown in DSC correlate with dehydration; both peaks in DSC (minor and major) are present at the same temperature as their respective dehydration phases. The conductivity graph shows interesting results. Superprotonic activity is not accurately portrayed in the heating phase, but the cooling phase does not deviate from common behavior. Due to hysterisis, the compound exhibits superprotonic conductivity at a lower temperature during cooling than its actual superprotonic temperature. In other words, the compound exhibits superprotonic behavior at a lower temperature in the cooling phase because it transitioning from a high conductive state to a low conductive state. Superprotonic activity is, by definition, acute increase in conductivity with increase in temperature, not decrease.

4.2 – **Discussion**

Based solely on our data accrued during the study, $Cs_5H_3(SO_4)_4$ shows enormous potential for the renewable energy field. $Cs_5H_3(SO_4)_4$ holds exciting potential in the renewable energy field as it has shown prevalent conductivity at lower temperatures. As per integration in fuel cells, the independence from a water management system provides solid acid fuel cells a noteworthy benefit over conventional fuel types and this independence itself validates attention to SAFCs as well as Cs_5-. Furthermore, the integration of $Cs_5H_3(SO_4)_4$ should not be limited only fuel cells, but any market that calls for high proton conductivity, such as in supercapacitors, as its viability as a high proton conductor has been successfully proven.

Our work on $(Cs_{0.95}Rb_{0.05})_5H_3(SO_4)_4$ indicates much promise but still leaves many questions unanswered. Exact behavior is still questionable and must be replicated with repeated tests before it can be confirmed that dehydration and phase changes occur. Our research on $(Cs_{0.95}Rb_{0.05})_5H_3(SO_4)_4$ leaves a strong basis for future studies as it alludes to superprotonic

conductivity at an even lower temperature. Furthermore, it encourages experimentation with "hybrid" compounds as they may yield benefits of two different compositions. Such compounds could eventually lead to the discovery of an even more efficiently functioning sample.

Because our study only covers a very narrow scope of not only the fuel cell field, but in electrolytes themselves, many questions remain unanswered. In terms of integration into fuel cells, how is conductivity affected over long durations of time? How does dehydration affect the conductivity? Several implications leave us attempting to piece together a very large puzzle. Why exactly does rubidium integration decrease superprotonic temperature and increase dehydration? Previous studies lack explanation of behavior at an atomic level; beyond the explanation of reorienting sulfate groups, very little data is published explaining the behavior of Cs_5-. Furthermore, other studies have identified problems regarding further application into fuel cells. The most severe of these problems is the impact of the H_2S by-product on the electrocatalyst. The reduction of the electrolyte induces the release of compounds such as H_2S which greatly alter the functioning of fuel cell performance [1]. Such problems can be expected to arise as more direct integration into fuel cells is investigated.

In conclusion, our work has developed a much more efficient synthesis method and sparked much curiosity for Cs_5-'s integration into fuel cells as well as experimentation of our $(CsRb)_5$- compound. Our $(CsRb)_5$- sample presents several interesting and unexplained qualities that require further exploration. Through our analysis and results in this study, it is evident that Cs_5- and $(CsRb)_5$- hold great potential in their behavior. If successfully integrated, these compounds could ultimately serve to help harvest energy in today's increasingly demanding civilization.

REFERENCES

3% Deficiency [1]

2% Deficiency

Haile, S.M.,"Fuel cell materials and Components" Acta Materialia, Volume 51, Issue 19, The Golden Jubilee Issue. Selected topics in Materials Science and Engineering: Past, Present and Future, 5981-6000 (2003).

3% Deficiency

[2]

Boysen, D.A., Uda, T., Chisholm, C.R.I., and Haile, S.M. "High-Performance Solid Acid Fuel Cells Through Humidity Stabilization" Science, 303.5654, 68-70 (2003).

Reference

[3]

Fukami, T., Jin, S., and Chen, R. H. "Studies of structure, thermal, and electrical properties for Cs5H3(SO4)4 crystal." Ionics, 5th ser. 12.4, 257-62 (2006).

[4]

Baranov, A.I., Sinitsyn, V.V., Vinnichenko, V.Y., Jones, D.J., and Bonnet, B. "Stabilisation of disordered superprotonic phases in crystals of the M5H3(AO4)4 xH2O family." Solid State Ionics, 97, 153-60 (1997)

[5]

Muroyama, H., Kudo, K., Matsui, T., Kikuchi, R., and Eguchi, K. "Electrochemical properties of MH2PO4/SiP2O7-based electrolytes (M = alkaline metal) for use in intermediate-temperature fuel cells." *Solid State Ionics,* **178**, 1512-516 (2007).

[6]

Fietz, T., Buchkremer, H., and Stöver, D. "Components manufacturing for solid oxide fuel cells." *Solid State Ionics,* **152-153**, 373-81 (2002).

[7]

Cowan, L.A ., Morcos, R.M., Hatada, N., Navrotsky, A., and Haile, S.M., "High temperature properties of Rb3H(SO4)2 at ambient pressure: Absence of a polymorphic, superprotonic transition." *Solid State Ionics,* **179,** 305-13 (2008).